Electronic Supplementary Material (ESI) for Nanoscale.

Supporting Information

Multicompartment Dendrimicelles with Binary, Ternary, and Quaternary Core Composition

Rebecca Kaup,[1,‡] Jan Bart ten Hove,[1,2,‡] Anton Bunschoten,[1] Fijs W. B. van Leeuwen,[1,2] and Aldrik H. Velders[1,2,3*]

Table of Contents

Experimental Procedures

Materials & Methods

Amine-terminated poly(amidoamine) (PAMAM) dendrimer generation 6 was obtained from Dendritech Inc, USA, as methanolic solutions. Rhodamine B isothiocyanate, 1M NaOH and HCl were obtained from Sigma Aldrich. $HAuCl_4.3H_2O$, MOPS buffer and fluorescein isothiocyanate were obtained from TCI. $pMAA_{64}$-b-PEO_{885} (Mw/Mn = 1.15) was obtained from Polymer Sources Inc., Canada, and used as a 5 mM solution based on carboxylic acid content. NaOD, DCl and D_2O with purity of 99.96 %D were obtained from Eurisotop, France.

For cryoTEM, samples were cast on Quantifoil R2/2 grids or 400 mesh Holey Carbon grids obtained from Electron Microscopy Sciences (EMS, Hatfield, USA) which were rendered hydrophilic using a plasma cleaning setup (~20 s at 10^{-1} Torr). After blotting, samples were plunged into a liquid ethane or ethane/propane mixture at ~liquid nitrogen temperature using a Vitrobot system (FEI Company).[1] Samples were imaged at ~100K in a JEOL 1400Plus TEM operating at 120 kV. TEM images were analyzed using FIJI (https://fiji.sc/).

Dynamic Light Scattering (DLS) was done on a Malvern Zetasizer Nano S, equipped with a 633 nm laser. Critical Micelle Concentrations were calculated by isotonic dilution of the dendrimicelle sample with MOPS buffer solution.

Nuclear Magnetic Resonance (NMR) spectra in D_2O were obtained on a Bruker Avance III spectrometer operating at 500 MHz for 1H, equipped with a 5 mm TXI probe. Deuterated trimethylsilylpropanoic acid (TMSP-d4) was used as internal standard at a concentration of 1 mM. Dendrimer concentrations were calculated by relating the integral of Bb protons of the dendrimer (δ = 2.27 – 2.47 ppm; 504, 1016, and 2040 protons for PAMAM G5, G6, and G7 respectively) to the integral of TMSP-d4 (9 protons).[2, 3]

A Hitachi U-2010 UV-Visible Spectrophotometer was used to measure UV-Visible absorbance spectra. The average number of fluorophores per dendrimer were calculated from UV-Visible absorption spectra using the Lambert-Beer law, taking $73x10^3$ respectively $106x10^3$ as the extinction coefficients for fluorescein respectively rhodamine B. Fluorescence excitation and emission spectra were acquired on Cary Eclipse spectrophotometer. Quantum yields were calculated in a relative way, using Rhodamine 6G (QY = 0.95 in ethanol) as standard.

The FRET efficiency (E) was calculated according to a method reported elsewhere.[4] For every FRET sample (f), two additional control samples were prepared for bleed-through corrections, containing either only the donor (d) or only the acceptor (a) molecule. Three different filter sets were used in steady-state spectroscopy. The donor filter set (D, excitation: 480 nm; emission integral: 500-540 nm), acceptor filter set (A, excitation: 480 nm; emission: 575-615 nm) and FRET filter set (F, excitation: 480 nm; emission integral: 575-615 nm). From this a letter code was created. The small letter describes which molecules are present and the capital letter describes the filter set. “Dd” would therefore refer to the donor-only sample measured with the donor filter set. The FRET efficiencies are then calculated using the following equations:

$$\mathrm{Af}^* = \frac{\mathrm{Af} - \left(\frac{\mathrm{Ad}}{\mathrm{Fd}}\right)\mathrm{Ff}}{1 - \left(\frac{\mathrm{Fa}}{\mathrm{Aa}}\right)\left(\frac{\mathrm{Ad}}{\mathrm{Fd}}\right)} \quad (1)$$

$$\mathrm{FRET1} = \frac{\mathrm{Ff} - \left(\frac{\mathrm{Fd}}{\mathrm{Dd}}\right)\mathrm{Df} - \mathrm{Af}^*\left[\left(\frac{\mathrm{Fa}}{\mathrm{Aa}}\right) - \left(\frac{\mathrm{Fd}}{\mathrm{Dd}}\right)\left(\frac{\mathrm{Da}}{\mathrm{Aa}}\right)\right]}{\mathrm{G}\left[1 - \left(\frac{\mathrm{Da}}{\mathrm{Fa}}\right)\left(\frac{\mathrm{Fd}}{\mathrm{Dd}}\right)\right]} \quad (2)$$

$$\mathrm{Df}^* = \mathrm{Df} + \mathrm{FRET1}\left[1 - \mathrm{G}\left(\frac{\mathrm{Da}}{\mathrm{Aa}}\right)\right] - \mathrm{Af}^*\left(\frac{\mathrm{Da}}{\mathrm{Aa}}\right) \quad (3)$$

$$\mathrm{E} = \frac{\mathrm{FRET1}}{\mathrm{Df}^*} \quad (4)$$

With Af^* and Df^* the acceptor and donor signal in the FRET sample when no FRET would take place, and FRET1 the loss of donor signal due to FRET. All samples of a single set of related experiments were measured on the same day, and without temperature control. It is good to note that exploiting this donor molecule, we avoid any interference with possible non-traditional intrinsic luminescence (NTIL).[9]

General Procedure for Fluorophore Labelling of PAMAM Dendrimers

Functionalization of amine-terminated PAMAM dendrimers with fluorophores was done using isothiocyanate chemistry. Shortly, 200 µL of PAMAM stock solutions (5% wt in MeOH, ~8 mg) were diluted to a total volume of 2 mL MeOH. Next, 4-8 equivalents of reactive dye (1 $mg.mL^{-1}$ of fluorescein- or rhodamine B-isothiocyanate in MeOH) were prepared and added slowly to the dendrimer solution. The final volume was set to 3 mL MeOH and the solutions were left to stir overnight. Afterward, MeOH was removed under reduced pressure, and the dendrimers were dissolved in distilled water. The functionalized dendrimers were purified by extensive dialysis against 3x 3L of demineralized water using Spectra/Por Float-A-Lyzer G2 dialysis tubes with a MWCO of 2.5-3.5 kDa. All experiments presented in this article were done with the same batch of functionalized dendrimers.

Dendrimer-Encapsulated Nanoparticles

G6-dendrimer-encapsulaed gold nanoparticles, G6-Au were made following established protocols as reported before.[5-8] Briefly, 50 µL PAMAM (5% wt in MeOH, ~2 mg) was evaporated under reduced pressure and dissolved in 2 mL of distilled water. After adjusting the pH to 3 using 1 M HCl, 1 mL of a 4.4 mM aqueous solution of $HAuCl_4$ was added (corresponding to a dendrimer loading of ~50% with respect to the number of dendrimer end groups). This solution was then stirred for 20 min, and 44 µL of a 1 M solution of $NaBH_4$ in 0.3 M NaOH (~10 molar equivalents to Au^{3+}) was added. Reduction of Au^{3+} to AuDENs was indicated by the change from ~colorless to a dark brown solution within seconds after addition. After stirring overnight, the pH was set to 7 using HCl, and the G6-Au were stored at 4 °C.

Dendrimicelle formation

Dendrimicelles were made under charge stoichiometric conditions by dissolving 20 µL of 2.9 mM dendrimer solution (charge concentration, based on surface groups) in 149 µL water. For all experiments the total amount of dendrimer was kept constant at 20 µL 2.89 mM solution, while varying the ratio between the different dendrimers. Next, 20 µL of 0.2 M MOPS buffer at pH 7.0 was added. Then, 11 µL $pMAA_{64}$-*b*-PEO_{885} (~55 nmol based on $–COO^-$) was added followed by sonication for 2 min. Samples were left to equilibrate for one day before characterization. Thiol-induced etching of dendrimer-encapsulated nanoparticles was done by adding ≥6 times excess of thiol to gold (—SH:Au(0)).

Results and Discussion

Dendrimer functionalization and characterization

Table S1. Overview of the fluorophore-functionalized dendrimers and their spectral characteristics. ^{1}H-NMR indicates an average of 4 fluorophores per fluorescein-functionalized dendrimer, and 2 fluorophores per rhodamine B-functionalized dendrimer. For the calculations the integral of the Bb peak, corresponding to 1016 H-atoms, and the integral of all fluorophore peaks in the aromatic range were used. This corresponds to nine H-atoms for both FITC and RITC. This was done to include all variations in the peaks caused by statistical distribution of the fluorophores on the dendrimers. *Note: the quantum yield of the fluorophores inside the dendrimicelles was ~17% for micelles made from G6-F, and ~3% for micelles made from G6-R. This slight decrease can likely be attributed to additional losses due to scattering of the micelles.

Dendrimer	Fluorophores	Average Fluorophores per dendrimer	Quantum Yield	Absorption Maximun (nm)	Excitaion Maximun (nm)	Emission Maximum (nm)
G6-F	FITC	4	0.21	500	496	521
G6-R	RITC	2	0.06	557	560	581

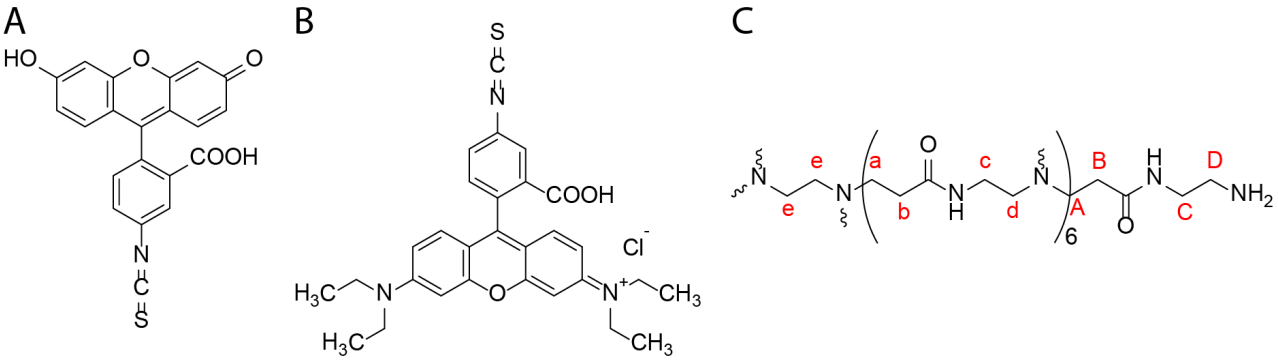

Figure S1. *Chemical structures of a) FITC, b) RITC and c) one branch of a PAMAM-NH2 generation 6 dendrimer.*

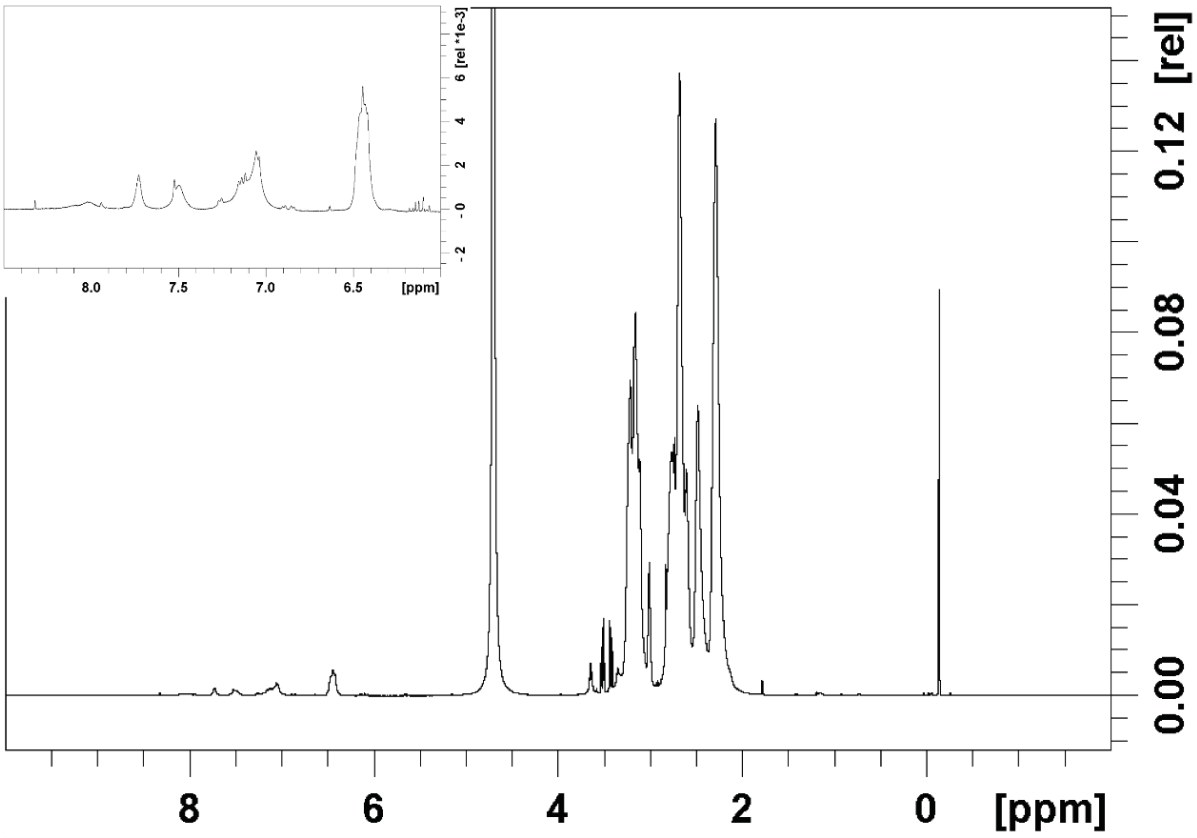

Figure S2. *NMR characterization of generation six PAMAM dendrimers functionalized with fluorescein isothiocyanate. The inset shows a magnification of the fluorophore region. Due to statistical distribution of the fluorophores on the dendrimers, line broadening and overlap of differently shifted peaks occurred.*

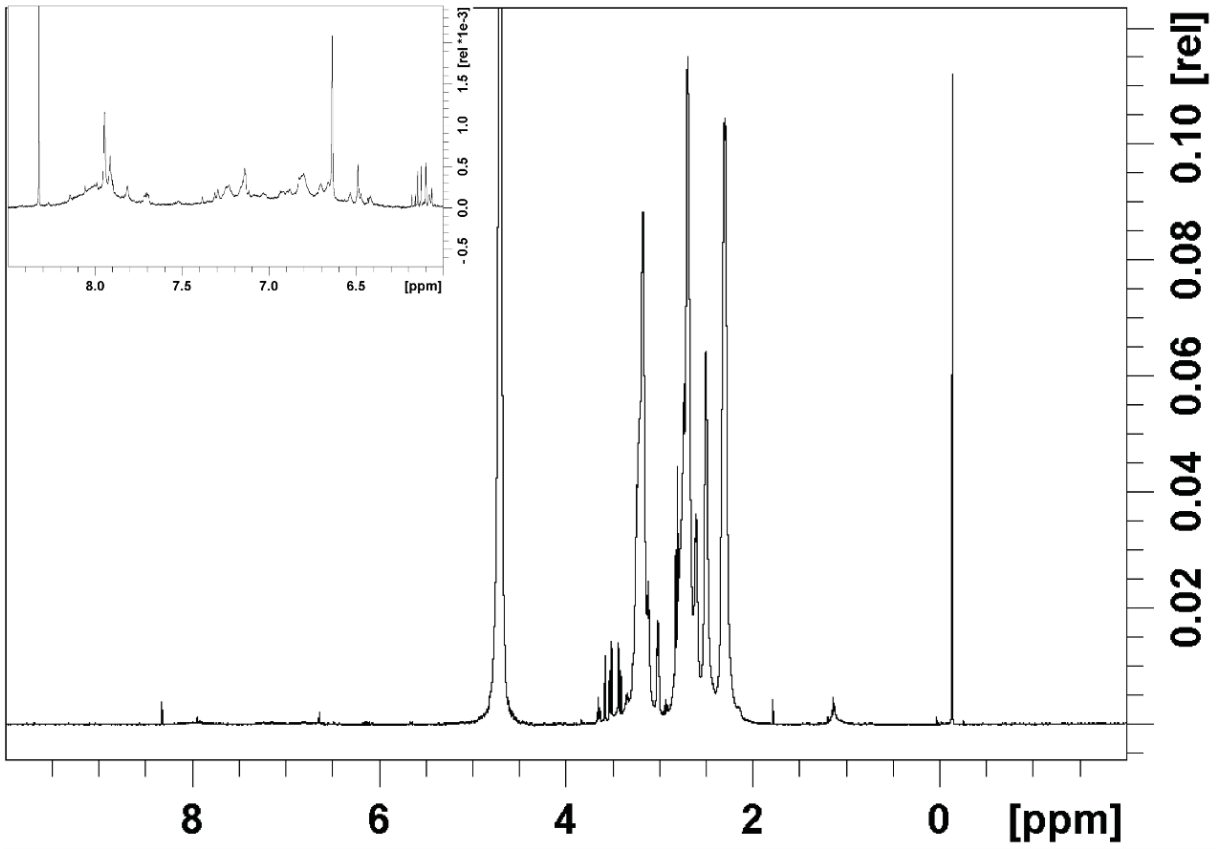

Figure S3. *NMR characterization of generation six PAMAM dendrimers functionalized with rhodamine B isothiocyanate. The inset shows a magnification of the fluorophore region. Due to statistical distribution of the fluorophores on the dendrimers, line broadening and overlap of differently shifted peaks occurred.*

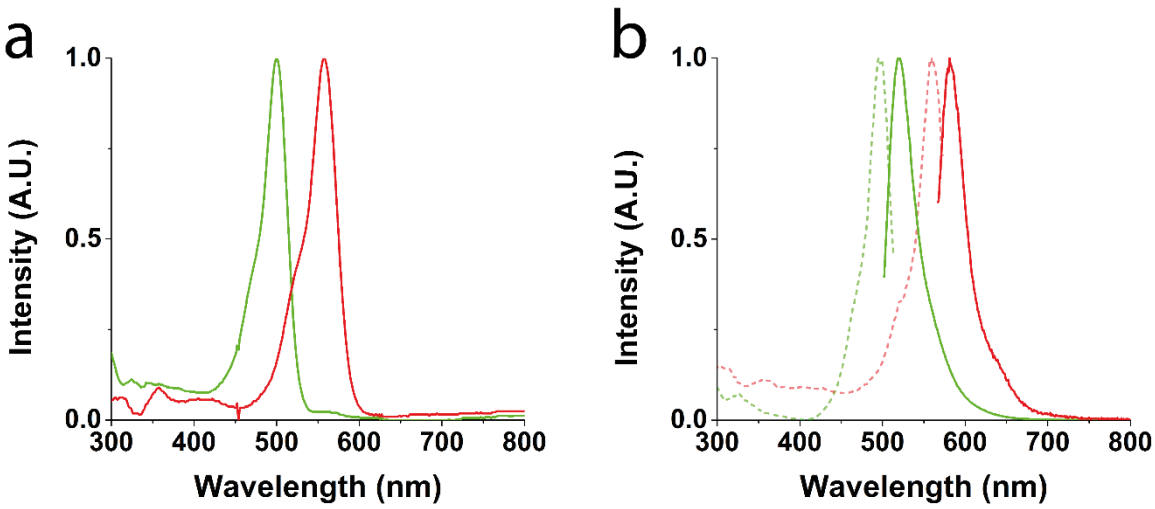

Figure S4. *Spectral characterization of fluorophore-functionalized dendrimers. a) UV-Visible absorption spectra of PAMAM dendrimer generation six functionalized with fluorescein (green) or rhodamine B (red) fluorophores. b) Excitation (dashed) and emission (solid) spectra of fluorophore functionalized PAMAM dendrimer generations six.*

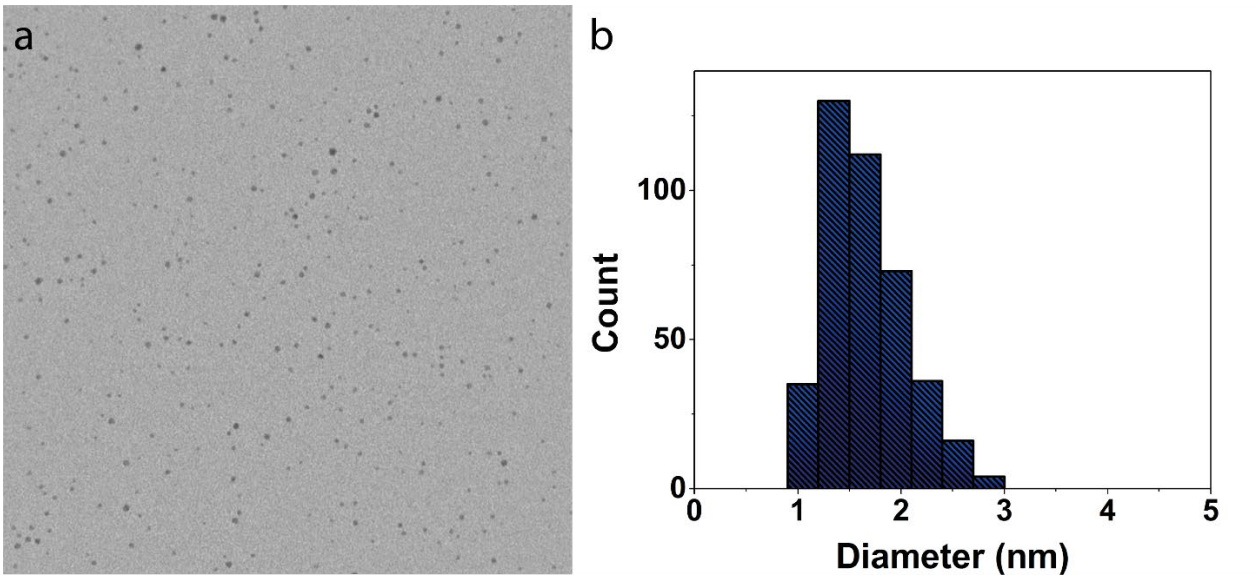

Figure S5. *(a) Transmission Electron Microscopy images of PAMAM G6-Au_{128} dendrimer-encapsulated gold nanoparticles. The scale bar represents 50 nm. (b) Size histograms of PAMAM G6-Au_{128} dendrimer-encapsulated gold nanoparticles. The average size is: 1.7 ± 0.4 nm. Note: the subscripts indicate the average number of gold atoms per nanoparticles. However, the nanoparticles are obtained in a statistical size distribution.*

I. Defining a binary FRET core micelle with fluorophore-functionalized dendrimers.

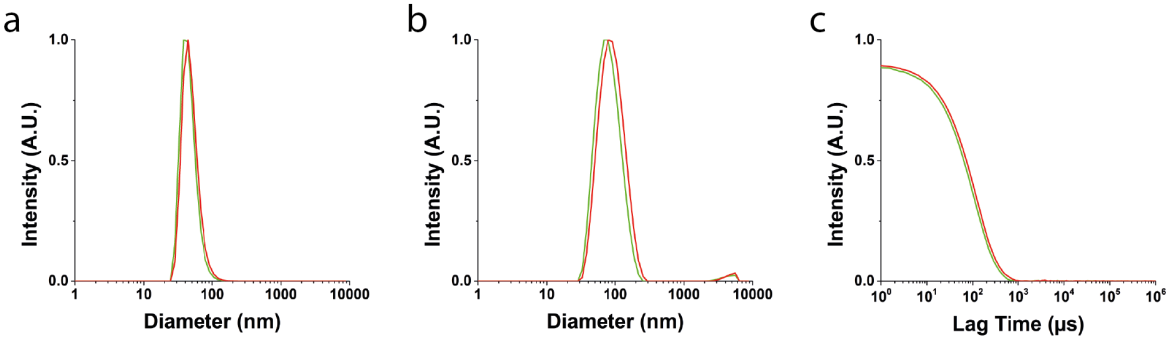

Figure S6. *DLS characterization of dendrimicelles made from fluorescein (in green) or rhodamine B (in red) functionalized dendrimers. a): Number-averaged size plots of G6-based dendrimicelles. The average micelle hydrodynamic diameter was determined to be ~47±2 nm. b): Intensity-averaged size plots of G6-based dendrimicelles. c): Correlograms of G6-based dendrimicelles, suggesting the absence of large aggregates.*

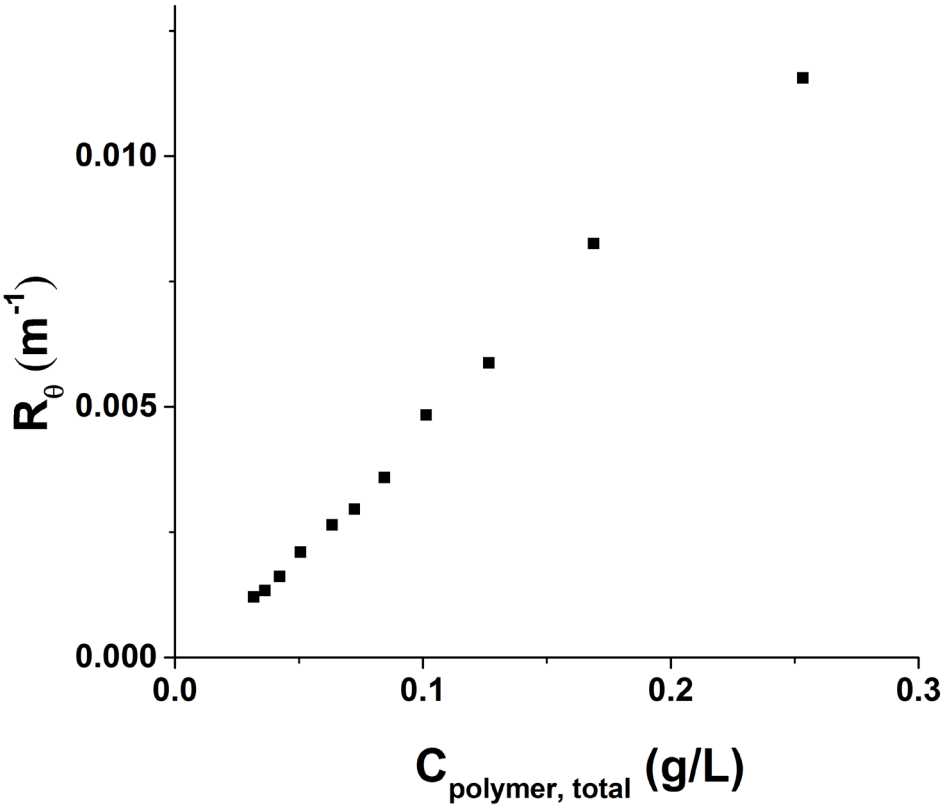

Figure S7. *Critical Micelle Concentration determination for dendrimicelles made from fluorophore-functionalized dendrimers. a) Dendrimicelles made from (1:1) G6-F:G6-R dendrimers have a CMC of ~1 mg.L^{-1}.*

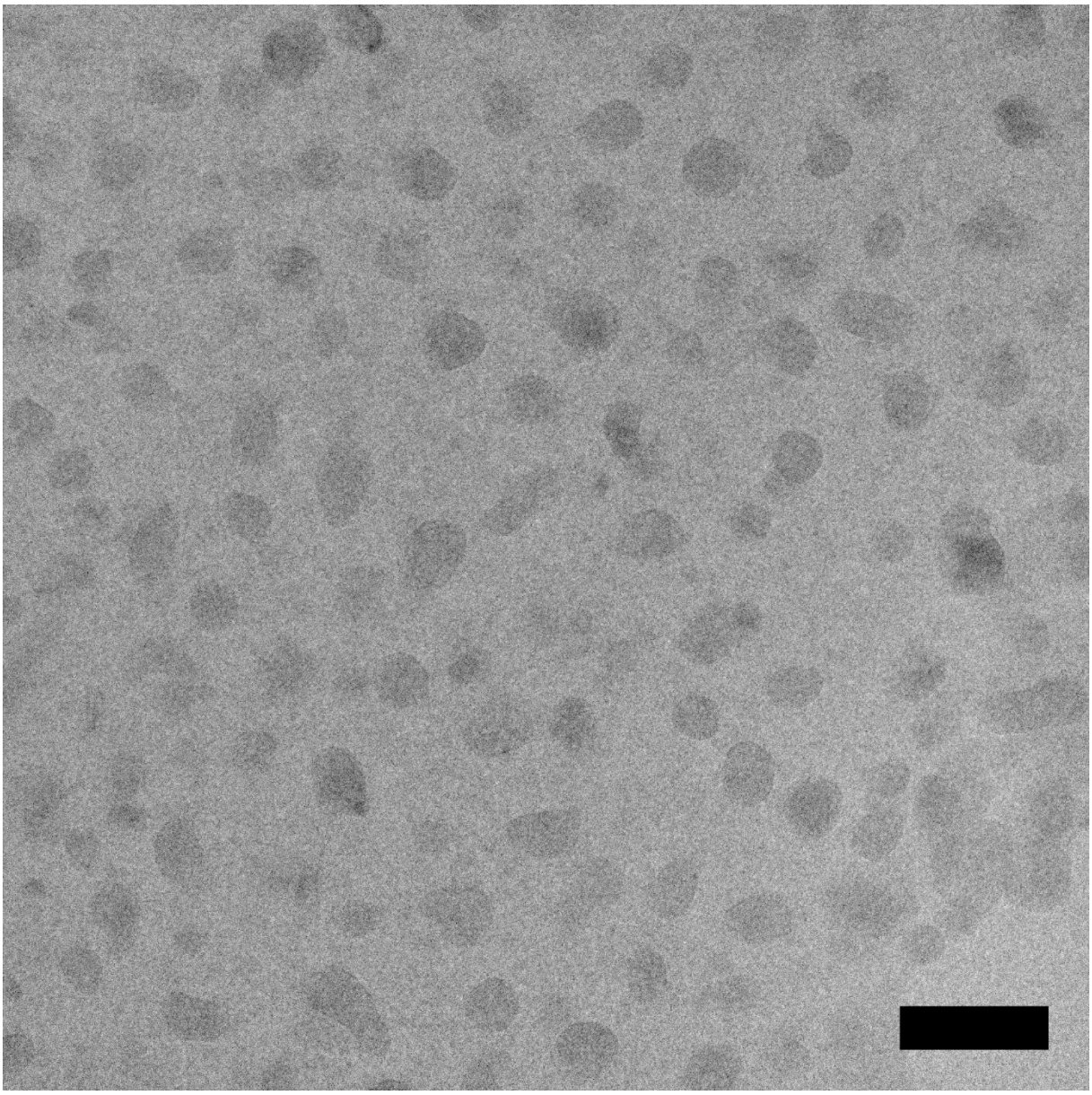

Figure S8. *Representative cryoTEM micrograph of charge-stoichiometrically made dendrimicelles from a (1:1) mix of G6-F and G6-R dendrimers. The scale bar represents 100 nm.*

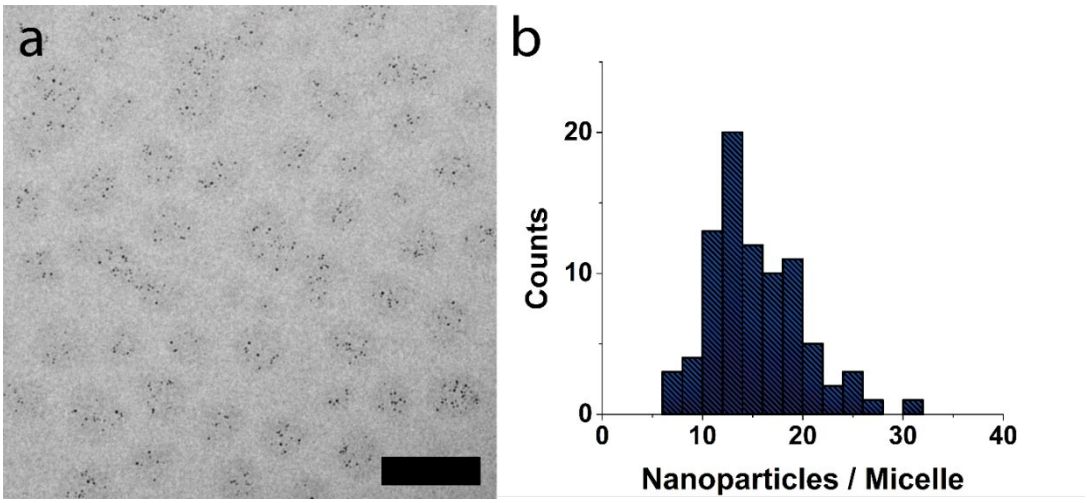

Figure S9. *Co-assembly of fluorophore-labelled and nanoparticle-containing dendrimers. a) cryoTEM micrograph of a dendrimicelle sample made from 1:1 mix of G6-F and G6-Au dendrimers. The scale bar is 100 nm. b) counting the number of nanoparticles per micelles reveals that the dendrimicelles contain an average of 15±5 nanoparticles per micelle, in perfect agreement with the expected values for dendrimicelles made from a 1:1 mix of 'empty' and nanoparticle-containing dendrimers, as we showed before that dendrimicelles made from only G6-Au dendrimers contain an average of 30±10 nanoparticles per dendrimicelle.*[7]

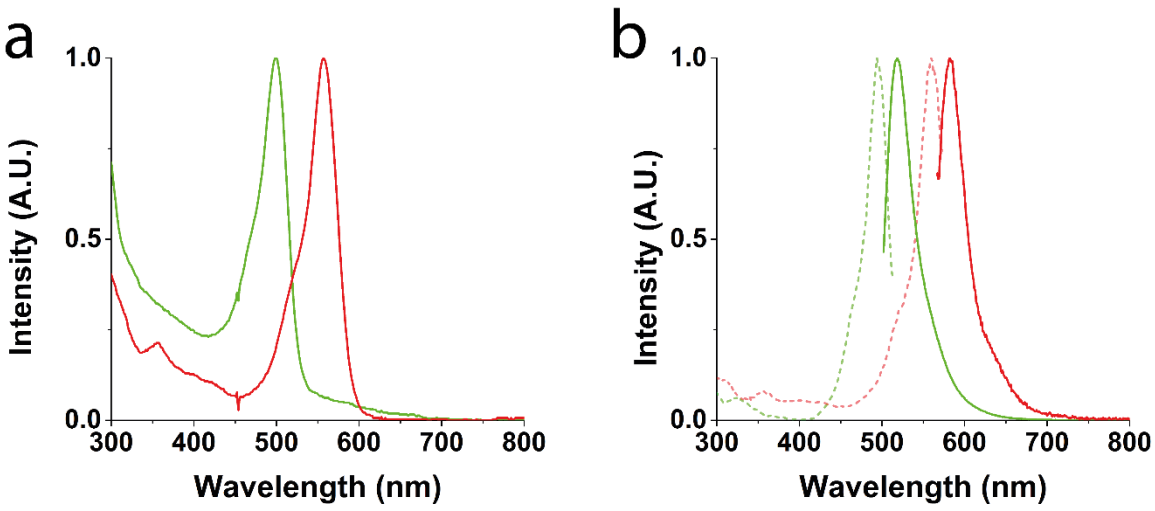

Figure S10. *Spectral characterization of micelles made from fluorophore-functionalized dendrimers. a) UV-Visible absorption spectra of dendrimicelles made from PAMAM generation six dendrimers functionalized with fluorescein (green) or rhodamine B (red) fluorophores. b) Excitation (dashed) and emission (solid) spectra of dendrimicelles made from fluorophore functionalized PAMAM dendrimer generations six. Emission spectra were recorded while exciting at λ=495 nm (fluorescein-functionalized dendrimers) or at λ=560 nm (rhodamine B-functionalized dendrimers). Excitation spectra were recorded by measuring the emission exciting at λ=520 nm (fluorescein-functionalized dendrimers) or at λ=580 nm (rhodamine B-functionalized dendrimers).*

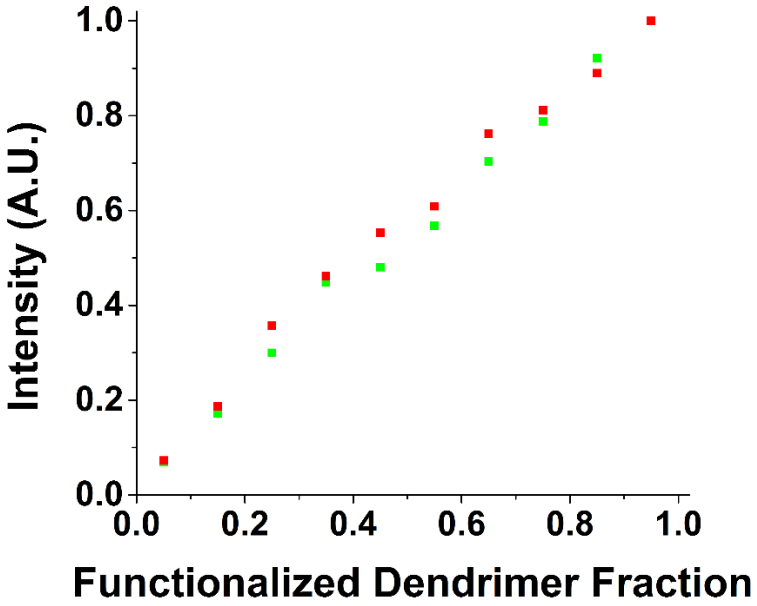

Figure S11. *Fluorophore emission versus fraction fluorophore-functionalized dendrimers. Generation 6- based dendrimicelles containing different ratios between G6-F and G6-E (green) or different ratios between G6-R and G6-E (red). G6-F and G6-E were excited at 480 nm. G6-R and G6-E were excited at 560 nm.*

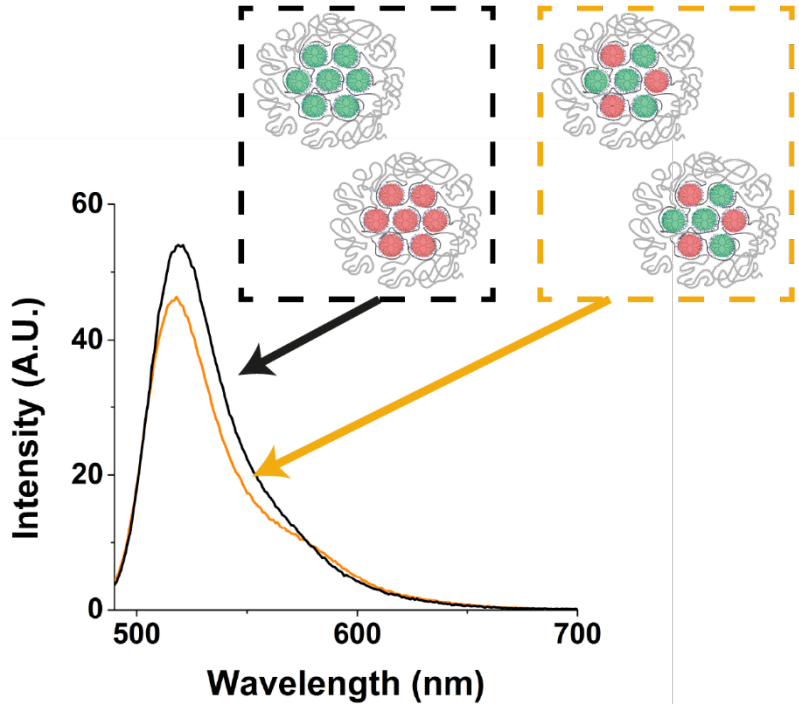

Figure S12. *Comparison of G6-based dendrimicelles made with fluorescein and rhodamine labelled dendrimers (orange), with a mix of dendrimicelles containing either only fluorescein labelled dendrimers or only rhodamine labelled dendrimers (black). The dendrimicelles containing both fluorophores show a decrease in donor signal (518 nm) and an increase in acceptor signal (580 nm), suggesting that FRET takes place within one micelle but not between micelles. The samples were excited at 480 nm.*

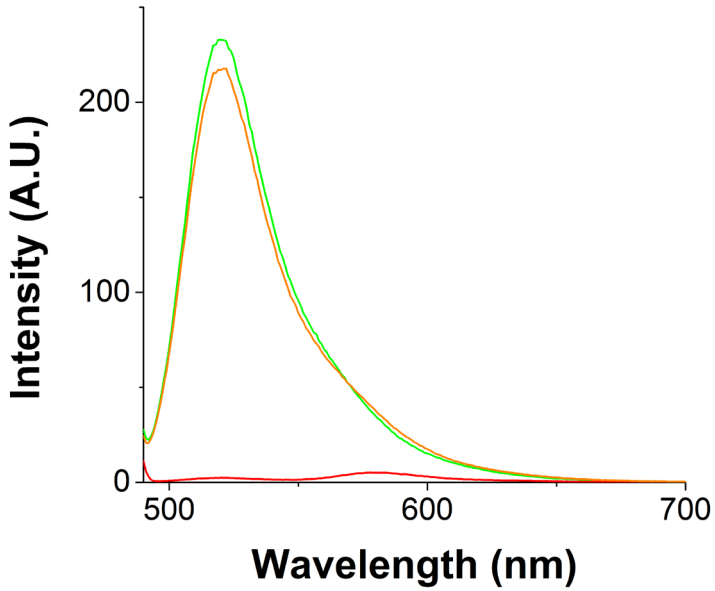

Figure S13. *Emission spectra of functionalized generation 6-based dendrimers excited at 480 nm. In green: fluorescein-functionalized dendrimers. In yellow: a 1:1 mix of fluorescein- and rhodamine B-functionalized dendrimers. In red: rhodamine B-functionalized dendrimers in solution. The determined FRET efficiency is <0.01.*

II. Quantitative Analyses of FRET aspects in binary and ternary-core dendrimicelles.

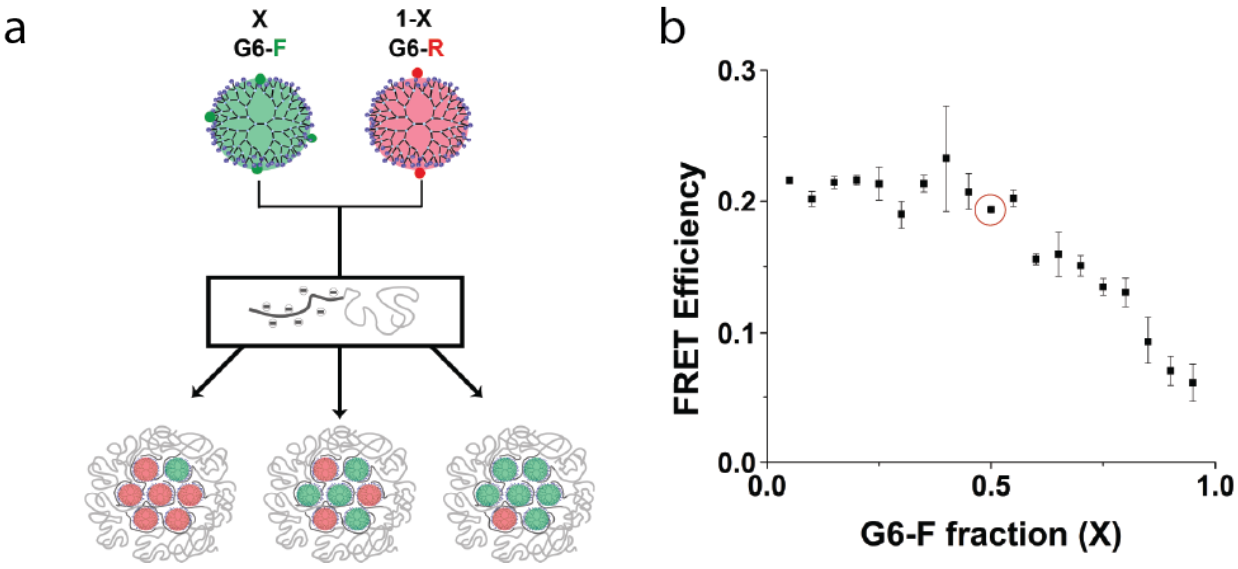

Figure S14: *Effect of the G6-F fraction on the FRET efficiency of the corresponding binary dendrimicelles. a) Scheme showing the binary-core dendrimicelle synthesis. The amount of G6-F (x) and G6-R (1-x) was varied while keeping the total dendrimer amount constant. b) FRET efficiency plot of samples from a). The FRET efficiency is roughly constant at ~0.2 up to a G6-F fraction of 0.5 (indicated with a red circle), whereas at higher G6-F fractions the FRET efficiency rapidly decreases.*

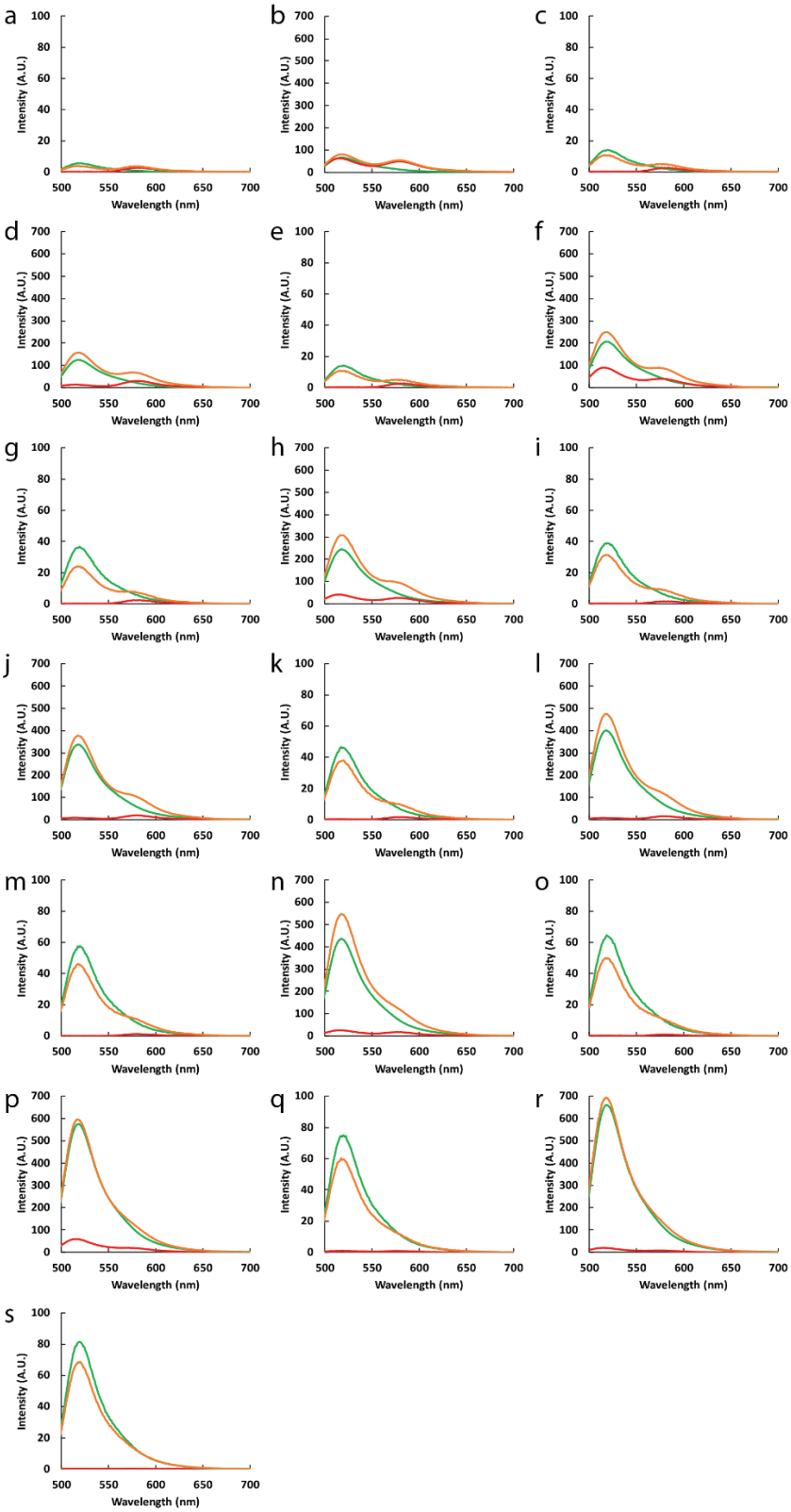

Figure S15. *Emission spectra of generation six-based dendrimicelles used for determining FRET efficiencies (Figure S15). Micelles made from (a-s): 5%, 10%, ...95% G6-F and 95%, 90%, ... 5% G6-E (green traces), 5%, 10%, ...95% G6-F and 95%, 90%, ... 5% G6-R (orange traces), and 5%, 10%, ...95% G6-E and 95%, 90%, ... 5% G6-R (red traces). Samples were excited at 480 nm. Samples with 10%, 20%,… were measured with a wider excitation slit than samples with 5%, 15%,… .*

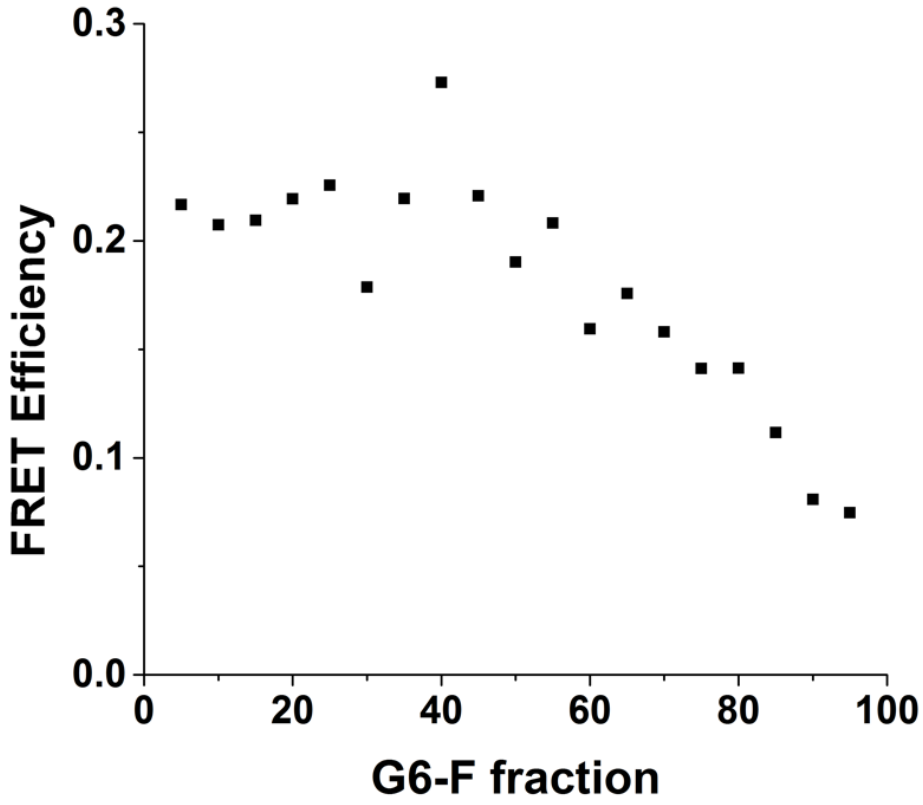

Figure S16. *FRET efficiencies of generation six-based fluorophore-containing dendrimicelles. The ratio between G6-F and G6-R was changed, keeping the number of dendrimers per micelle constant.*

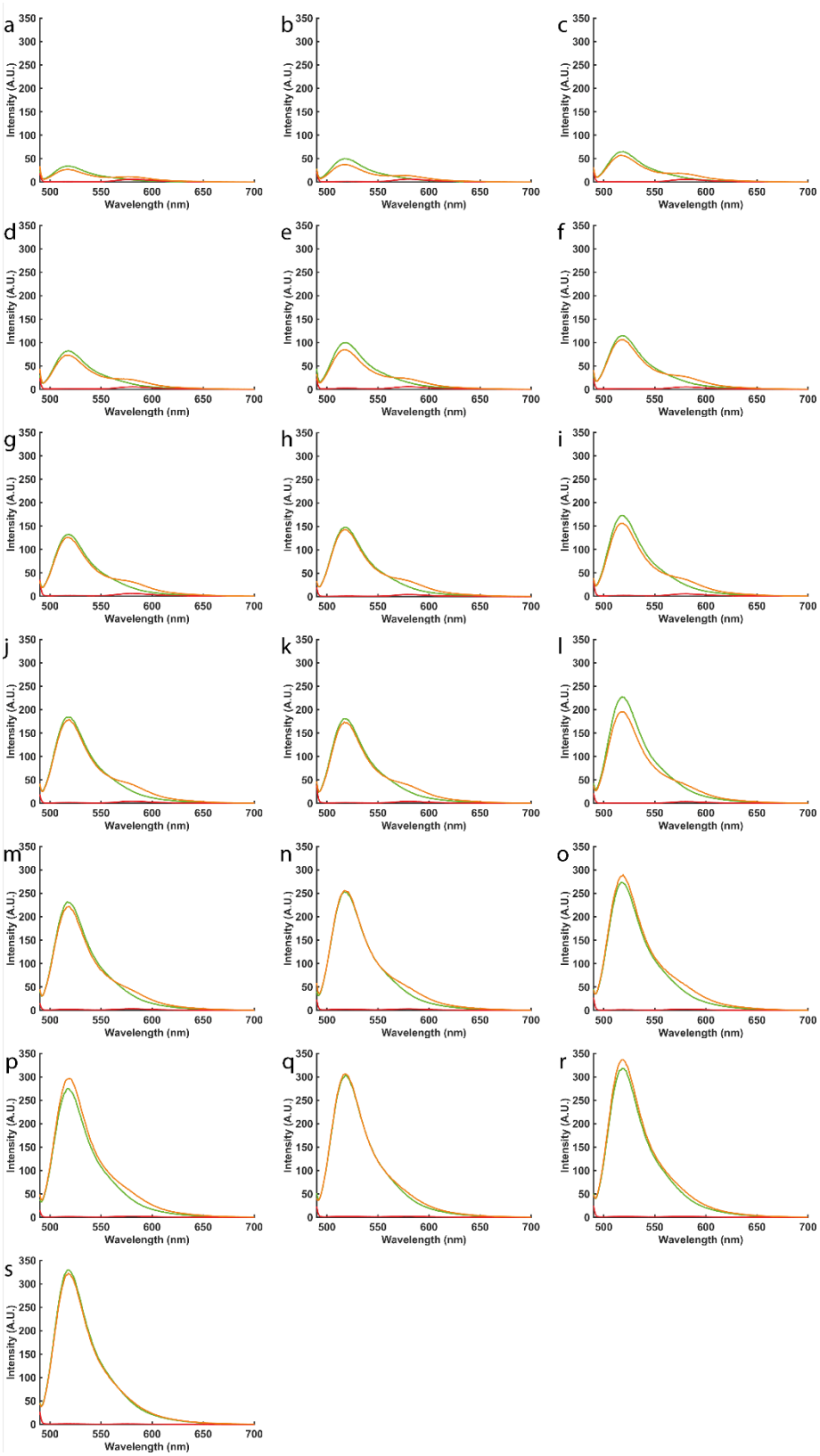

Figure S17. *Emission spectra of generation six-based dendrimicelles used for determining FRET efficiencies (Figure S17). Micelles made from (a-s): 5%, 10%, ...95% G6-F and 95%, 90%, ... 5% G6-E (green traces), 5%, 10%, ...95% G6-F and 95%, 90%, ... 5% G6-R (orange traces), and 5%, 10%, ...95% G6-E and 95%, 90%, ... 5% G6-R (red traces). Samples were excited at 480 nm.*

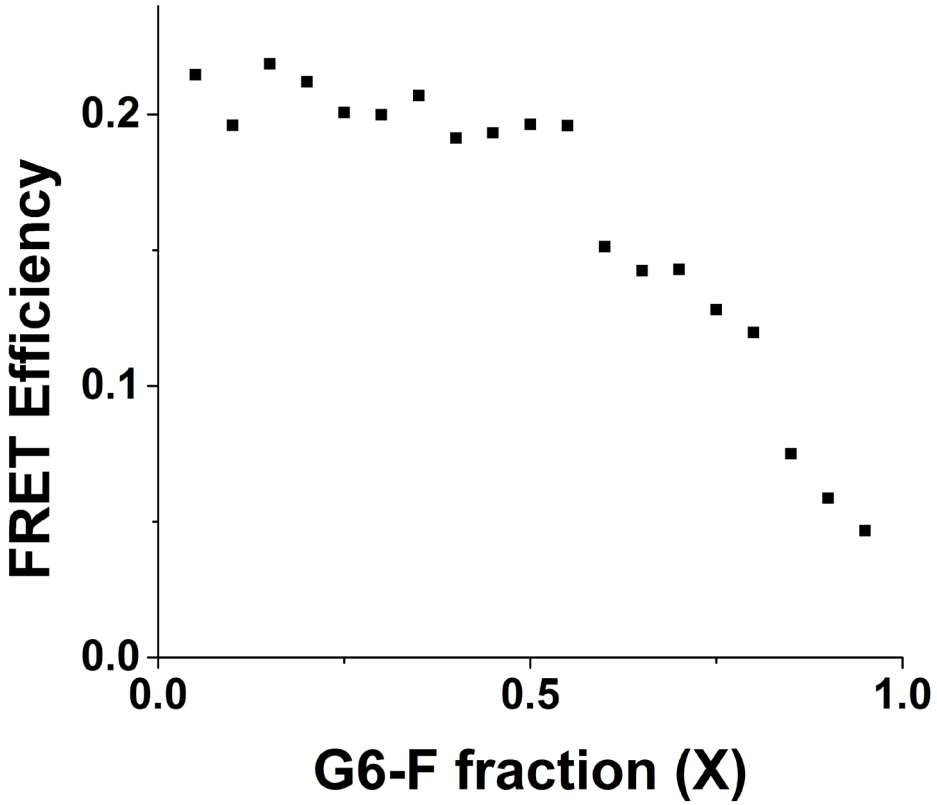

Figure S18. *FRET efficiencies of generation six-based fluorophore-containing dendrimicelles. The ratio between G6-F and G6-R was changed, keeping the number of dendrimers constant.*

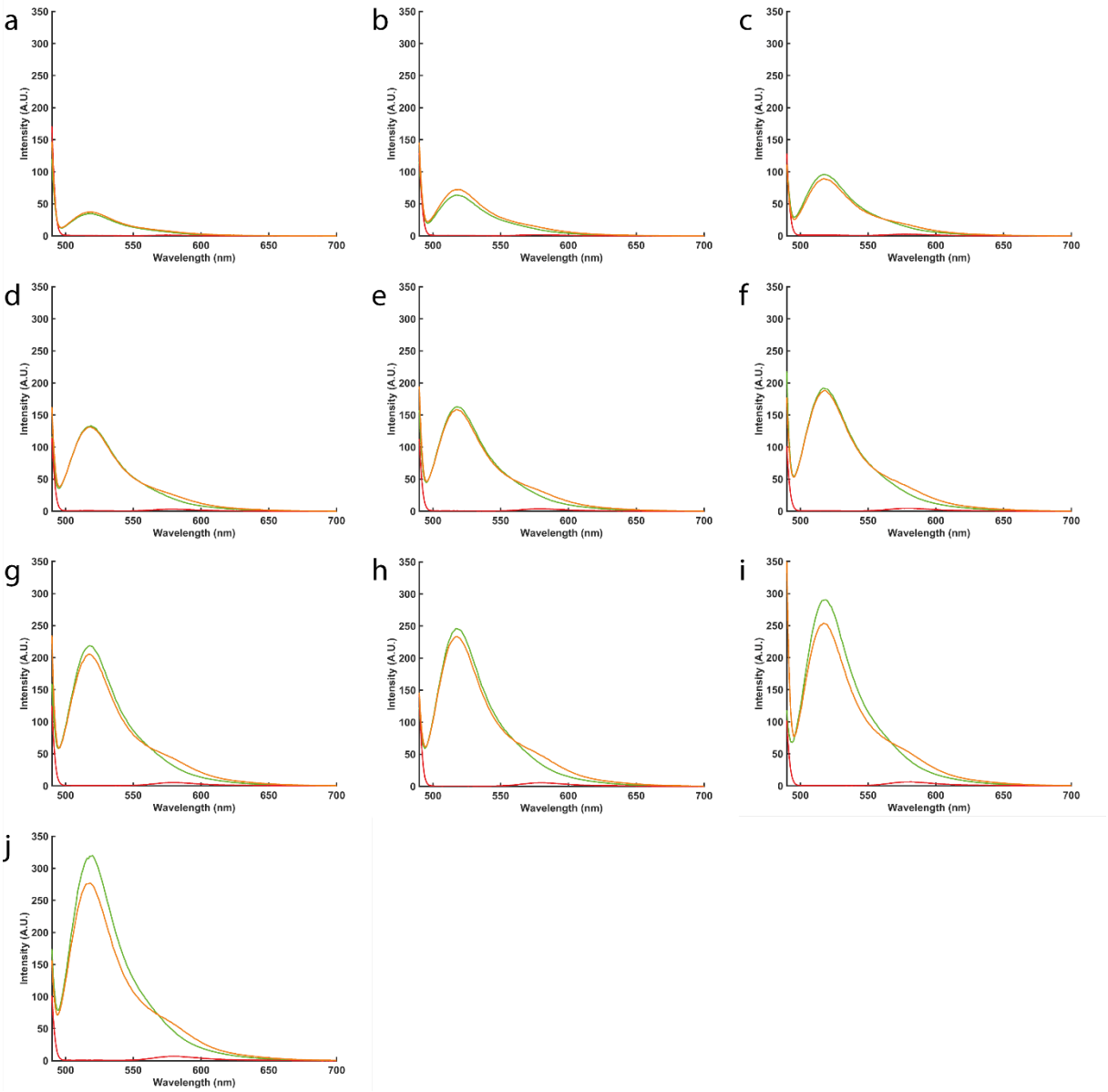

Figure S19. *Emission spectra of generation six-based ternary dendrimicelles used for determining FRET efficiencies in Figure 2d in the main text. Micelles made from (a-j): 5%, 10%, ...50% G6-F and 95%, 90%, ... 50% G6-E (green traces), 5%, 10%, ...50% G6-F and 5%, 10%, ... 50% G6-R and 90%, 80%, ... 10% G6-E (orange traces), and 5%, 10%, ...50% G6-R and 95%, 90%, ... 5% G6-E (red traces). Samples were excited at 480 nm.*

III. Dendrimicelles with gold nanoparticle-containing dendrimers, from binary and ternary to quaternary-core compositions.

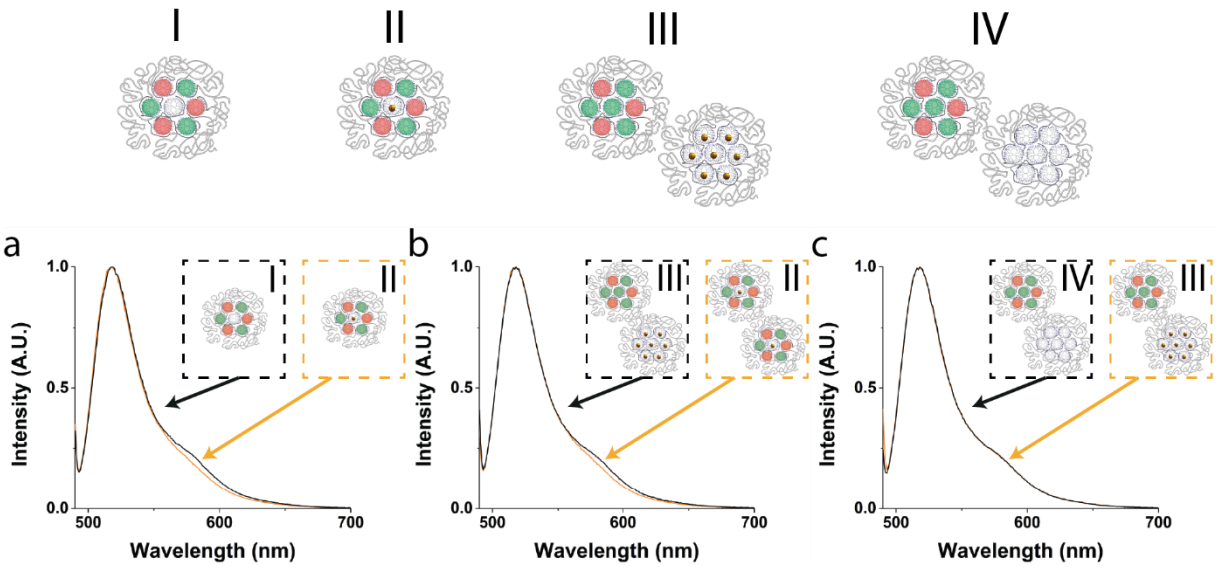

Figure S20. *a-c) Emission spectra of generation 6-based dendrimicelles. (a,) G6-FRE dendrimicelles (black) against G6-FRAu dendrimicelles (orange). The micelles containing empty dendrimers show a higher intensity in the acceptor region, around 580 nm, corresponding to a higher FRET efficiency; this corroborates that the AuNPS affect the FRET efficiency inside the micelles. (b) G6-FR and G6-Au (black) against G6-FRAu dendrimicelles (orange). The sample with a mix of G6-FR micelles and G6-Au micelles shows a higher intensity in the acceptor region, around 580 nm, corresponding to a higher FRET efficiency; also here the AuNPs affect the FRET efficiency only when present within the same micelle core as the FRET pair. (c) G6-FR and G6-E (black) against G6-FR and G6-Au dendrimicelles (orange). No difference is visible between the two samples, confirming that the AuNPs have no influence on the FRET efficiency of another micelle.*

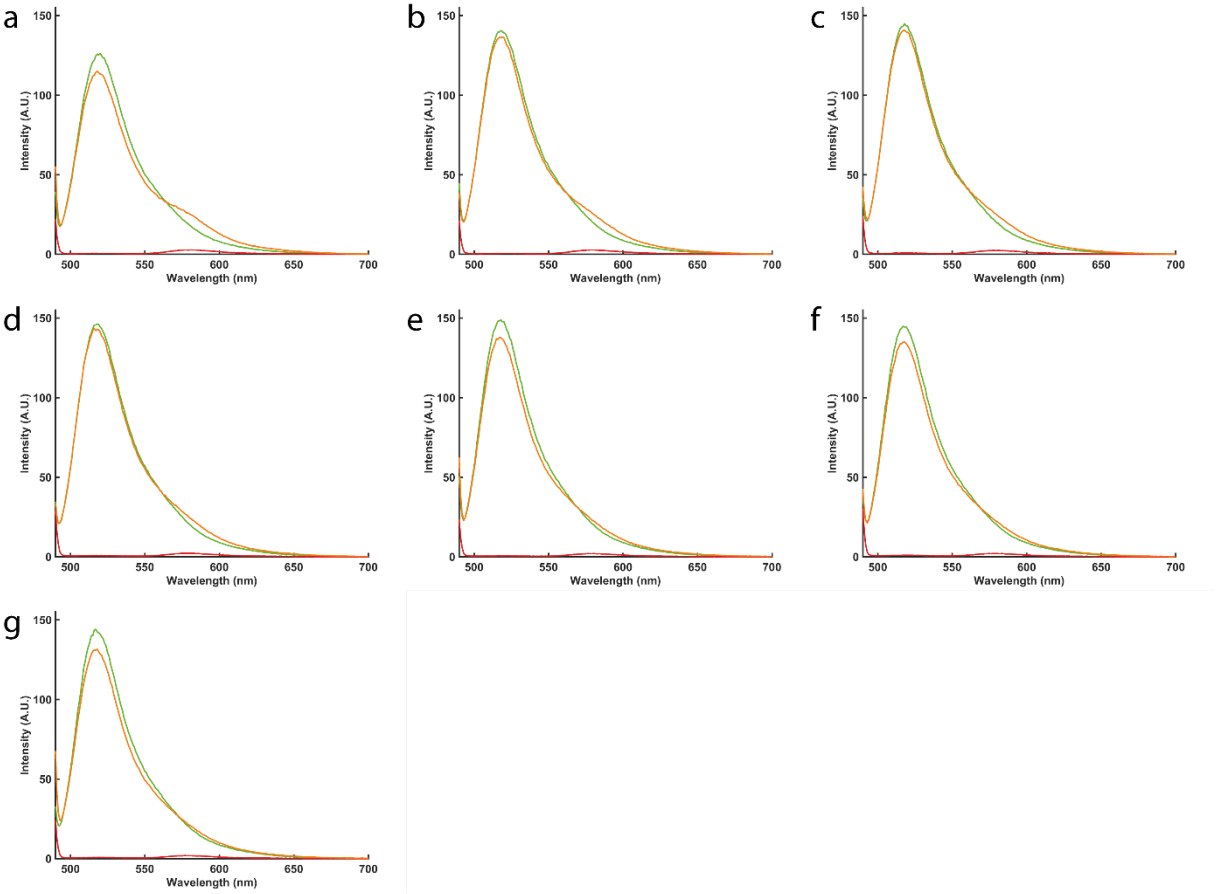

Figure S21. *Emission spectra of generation six-based quaternary dendrimicelles used for determining FRET efficiencies (G6-FRAuE, figure 3 in main text). Micelles made from (a-g): 35% G6-F and 65%, 60%, ... 35% G6-E and 0%, 10% ... 30% G6-Au (green traces), 35% G6-F and 35% G6-R and 30%, 25%, ... 0% G6-E and 0%, 5%, ... 30% G6-Au (orange traces), and 35% G6-R and 65%, 65%, ... 35% G6-E and 0%, 10% ... 30% G6-Au (red traces). Samples were excited at 480 nm.*

IV. Chemical responsiveness and tuning of the ternary-quaternary core composition.

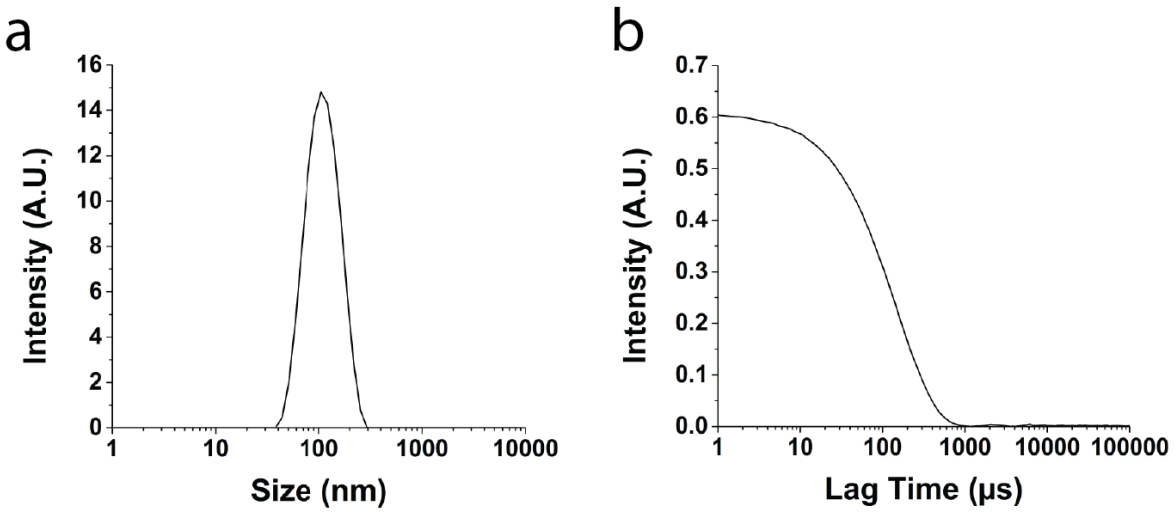

Figure S22. *Intensity- and Correlation plot of G6-FRAu containing 30% of G6-Au after addition of thiol, suggesting that the micelles are still intact.*

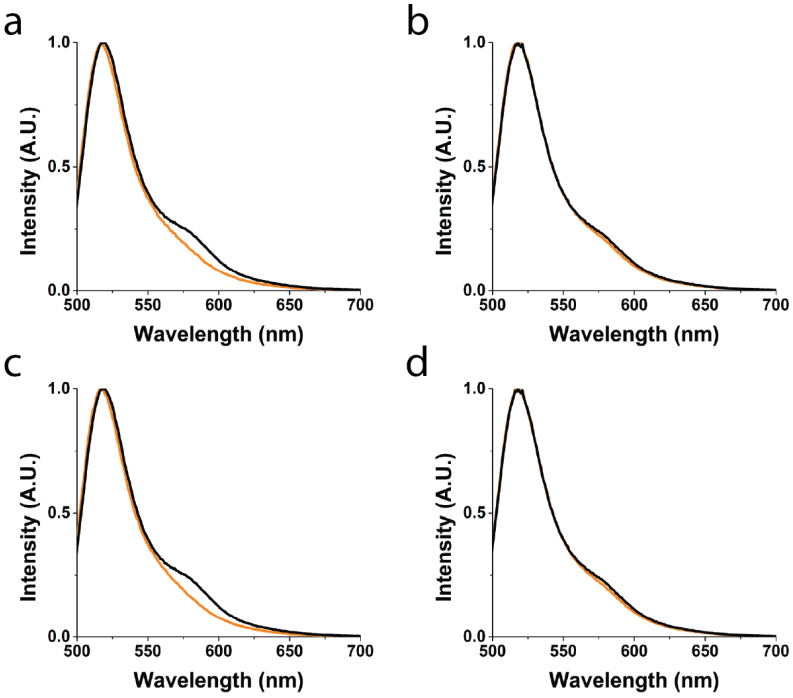

Figure S23. *Generation 6- based dendrimicelles. G6-FRAu dendrimicelles (orange) against G6-FRE dendrimicelles (black). All samples contain 35% G6-F, and 35% G6-R. The remaining 30% are either G6-E or G6-Au or both. a), b) G6-FRAu dendrimicelles containing 15% G6-Au. c), d) G6-FRAu dendrimicelles containing 30% G6-Au. The fluorescence emission was measured before (left) and after (right) incubation with ME. The samples were excited at 480 nm.*

References

1. W. F. Tivol, A. Briegel and G. J. Jensen, *Microscopy and microanalysis : the official journal of Microscopy Society of America, Microbeam Analysis Society, Microscopical Society of Canada*, 2008, **14**, 375-379.
2. V. M. Gomez, J. Guerra, S. V. Myers, R. M. Crooks and A. H. Velders, *Journal of the American Chemical Society*, 2009, **131**, 14634-14635.
3. V. M. Gomez, J. Guerra, A. H. Velders and R. M. Crooks, *Journal of the American Chemical Society*, 2009, **131**, 341-350.
4. G. W. Gordon, G. Berry, X. H. Liang, B. Levine and B. Herman, *Biophysical Journal*, 1998, **74**, 2702-2713.
5. J. B. ten Hove, J. Wang, F. W. B. van Leeuwen and A. H. Velders, *Nanoscale*, 2017, DOI: DOI: 10.1039/c7nr06773a.
6. J. B. ten Hove, J. Wang, M. N. van Oosterom, F. W. B. van Leeuwen and A. H. Velders, *ACS Nano*, 2017, DOI: 10.1021/acsnano.7b05541.
7. J. B. ten Hove, F. W. B. van Leeuwen and A. H. Velders, *Nature Communications*, 2018, **9**, 5207.
8. J. B. ten Hove, M. N. van Oosterom, F. W. B. van Leeuwen and A. H. Velders, *Scientific Reports*, 2018, **8**, 13820.
9. D. A. Tomalia, B. Klajnert-Maculewicz, K. A.-M. Joyhnson, H. F. Brinkman, A. Janaszewska, D. M. Hedstrand*, Prog. Polymer. Sci., 2019, **90**, 35-117.*